Carbon Black Filled Natural Rubber. 1. Structural Investigations

J. C. Kenny,† V. J. McBrierty,*,†,‡ Z. Rigbi,§ and D. C. Douglass‡

Department of Pure and Applied Physics, Trinity College, University of Dublin, Dublin 2, Ireland, AT&T Bell Laboratories, Murray Hill, New Jersey 07974, and Technion—Israel Institute of Technology, 32000 Haifa, Israel

Received March 12, 1990; Revised Manuscript Received July 9, 1990

ABSTRACT: This paper examines the effects of solvent extraction of increasing severity on carbon black filled natural rubber. Collated NMR (T_1, T_2, and $T_{1\rho}$), DSC, and DMTA methods examine the glass transition and motional cooperation in the filled system. DSC is insensitive to the immobilization of small amounts of tightly bound rubber on the surface of carbon black particles as detected in NMR line-width data. Also, examination of component T_2 intensity data as a function of temperature engenders the notion of a range of binding energies between the rubber and the carbon black. In particular, the mechanism for the progressive removal of bound rubber molecules appears to be Arrhenius in character. The Carr–Purcell pulse train has been used to glean additional insight into the dynamics of molecular motion, and exchange between heterogeneous sites is explored.

Introduction

The incorporation of carbon black into elastomers is a process of significant commercial importance,[1,2] and, despite considerable progress in understanding the ensuing morphology and molecular motions, certain aspects are still obscure. Indeed, the macromolecular motions in elastomers without filler above the glass transition are, in themselves, complex. Schaefer[3] deduced from differences in ^{13}C spin–lattice relaxation times (T_1) of individual carbons on the *cis*-1,4-polyisoprene (*cis*-PIP) chain that the main-chain segmental motions are anisotropic and deviate from true liquid-like behavior above T_g. The inapplicability of the extreme-narrowing condition was confirmed in Overhauser enhancement measurements. English and co-workers,[4,5] exploiting coherent averaging techniques to identify rates and amplitudes of motions in *cis*-1,4-polybutadiene (*cis*-PB), concluded that the residual line width at room temperature, of the order of a few hundred hertz, is due to rapid anisotropic segmental motion that is spatially inhibited by chain constraints. These observations are collectively consistent with the presence of chain entanglements as predicted in the comprehensive analysis of Cohen-Addad and co-workers.[6-8] VanderHart and co-workers[9] and Komoroski[10] give a general account of the origins of line broadening in ^{13}C spectra.

Schaefer noted further that $T_1(^{13}C)$ in *cis*-PIP was not noticeably affected by the incorporation of carbon black but that ^{13}C line widths increased by factors of between 5 and 10. Magic-angle spinning at 1 kHz induced line narrowing of the order of a factor of 4 in vulcanized carbon black filled *cis*-PIP.[11] Dybowski and Vaughan[12] also observed line broadening in proton resonance spectra in both filled and unfilled PIP which they attributed to anisotropic motions.

The results of selective saturation experiments led Schaefer to believe that neither micro- nor macroscopically inhomogeneous magnetic fields were the source of appreciable line broadening. He concluded that chain diffusion would have to be rapid to allow the ^{13}C nuclei to sample all values of inhomogeneous field to account for the observed homogeneous line widths. This ruled out observable effects due to local magnetic field or susceptibility variations. In the context of later discussion, however, it is important to note in these experiments that the carbon lines behave homogeneously on a time scale of T_1 but not necessarily so on shorter time scales such as T_2. Clearly also, the carbon black free radicals do not contribute significantly to the NMR response in this scenario. This latter result is in agreement with the calculated effects of local magnetic field gradients in carbon black filled *cis*-PB which demonstrate that the extremely short T_2 observed in the filled material is not due to these field gradients but arises from severe motional constraints experienced by the rubber molecules in the immediate vicinity of the carbon black particles.[13] Two other regions of characteristic T_2 behavior are detected in filled *cis*-PB in addition to this tightly bound layer. More loosely bound material is evident that exhibits vigorous, liquid-like motion but that is nonetheless constrained compared to the neat polymer, and there is material that behaves much like unfilled elastomer.[14,15] A model of the filled system has been constructed on the basis of these observations.[15]

A more recent study by Kentgens and co-workers[16] is at first sight at odds with some of these observations in concluding that the residual line width in *cis*-PIP is perhaps due to microscopic heterogeneities generated by the carbon black. These authors make two further observations: first, they detect a dependence of broadening on the laboratory field B_0, which is in conflict with results reported for *cis*-PB.[4,5] This field dependence implies some local susceptibility effects that do not depend on $P_2(\theta)$; that is, the sources of the susceptibility broadening are either nonspherical, nondilute, or inhomogeneous structures (or all three). Second, in a 2D exchange experiment[17] at room temperature they conclude that the ^{13}C chemical shift tensor does not reorient within a 40-ms time scale, which is consistent with English's picture[5] and not necessarily at odds with Schaefer's selective saturation experiments[3] because of the differing time scales.

The purpose of this paper is to refine the model developed earlier[15] to describe structural and motional heterogeneity in filled elastomers. Specifically, this work initiates an exploration of the response of natural rubber filled with HAF carbon black to extraction procedures of increasing severity, as reflected in solid-state NMR experiments. The expected progressive removal of loosely bound rubber should result in changes in the chain

* To whom correspondence should be addressed at the University of Dublin.
† University of Dublin.
‡ AT&T Bell Laboratories.
§ Technion—Israel Institute of Technology.

0024-9297/91/2224-0436$02.50/0

dynamics that become measurable when insight into the roles of temporal and spatial magnetic field fluctuations due to local susceptibility dispersion and dipolar interactions is established, as in the manner pioneered by Dybowski and Vaughan for untreated pure and filled rubber.

Experimental Section

Sample Preparation. The samples under investigation were prepared in the following manner. One hundred parts by weight of SMR5 grade of natural rubber were mixed on a laboratory mill with 50 parts of N330 carbon black supplied by Cabot Corp. as Vulcan 3 HAF. This grade of carbon black has a particle size index of 27 nm and an iodine absorption number of 82 mg/g according to ASTM D1510. The nominal surface area (A) and the density (ρ) are 86 m^2/g and 2.06 g cm^{-3}, respectively. SMR5 contains the following trace impurities: 0.05% particulate matter, 0.6% ash, 1% volatile matter, and 0.65% nitrogen as an indicator of the protein content of the rubber. A density of 0.97 g cm^{-3} is assumed for the natural rubber. The filled master batch sample was removed as a thin sheet, about 1 mm thick, and strips cut from it were subjected to various treatments in order to remove increasing quantities of rubber. Sample designations are as follows, where the numbers in parentheses denote the residual rubber/carbon black ratio: sample A, natural rubber as received; sample B, the original master batch containing a total rubber content equal to 200% of the carbon black content (2.0); sample C, mix B extracted for 7 days in three fresh lots of hexane at room temperature and then dried (0.662); sample D, a replicate of sample C (0.633); sample E, strips of sample C subsequently extracted in boiling hexane (342 K) under reflux for 8 h and then dried (0.592); sample F, strips of sample E extracted in boiling isooctane (≈398 K) for 8 hours (drying was accelerated by washing and decanting in hexane for four periods of 1 h) (0.461); sample G, strips from sample C extracted in boiling toluene (383 K) subsequently decanted and washed as for sample F (0.242); sample H, strips from sample C extracted in boiling mixed xylenes at ≈418 K (much of the sample disintegrated, but a few lumps were recovered and brought to constant weight by washing in hexane as for sample F) (unknown).

Data Acquisition and Analysis. NMR spin–spin (T_2), spin–lattice (T_1), and rotating-frame ($T_{1\rho}$) relaxation times were recorded on a Bruker spectrometer operating at a resonant frequency of 40 MHz for which a 90° pulse and recovery time were, respectively, 2.5 and 7 μs. Solid-echo[18] and spin-echo[19] sequences provided T_2 in the short and long relaxation time regimes as described earlier.[20] Data were fit to the Weibull function $\exp(-t/T_2)^E$, where E = 1 denotes Lorentzian (exponential) decay, and E = 2, Gaussian decay.[21,22] T_1 and $T_{1\rho}$ (B_1 = 10 G) were determined from the 180°–t–90°[17] and 90°–90° (phase shifted) spin-locking[23] sequences, respectively. Sample temperature was controlled to ±1 K.

DSC data were recorded and analyzed on a Perkin-Elmer DSC-4 differential scanning calorimeter interfaced to a thermal analysis data system. Thermograms were recorded at least twice to ensure reproducibility of results. The fusion peak of indium provided a reference for energy and temperature calibration. Sample weights were recorded to an accuracy of ±0.01 mg.

Mechanical loss data in the form of tan δ versus temperature over a frequency range 0.03–30 Hz were recorded on the computer-controlled dynamic mechanical thermal analysis (DMTA) system developed by Polymer Laboratories.

Results and Discussion

Representative T_1, $T_{1\rho}$, and T_2 data for samples A, B, E, and G are presented as a function of temperature in Figure 1. Results for natural rubber are in general accord with earlier observations[24] where relaxation behavior between 220 and 320 K manifests the glass-to-rubber transition, for which pertinent data are collated in Table I. Relaxation due to methyl group motion occurs at lower temperatures, outside the range of our measurements. The fact that the magnitudes of the observed minima are generally higher than theoretical predictions based on Mc-

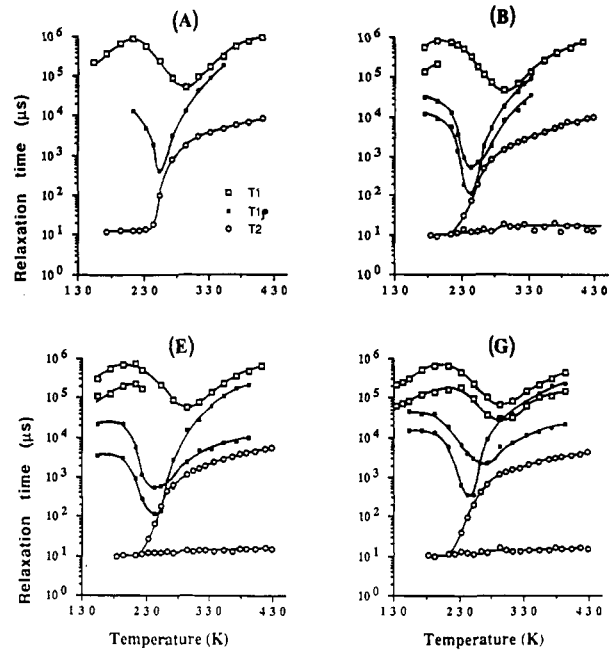

Figure 1. T_1 (□), $T_{1\rho}$ (■), and T_2 (○) data for the samples indicated.

Table I
NMR Glass Transition Data for Selected Samples

sample	$T_{1(min)}$ temp, K	$T_{1(min)}$ magnitude, ms	$T_{1\rho(min)}$ temp, K	$T_{1\rho(min)}$ magnitude, ms	T_{2L} transition temp, K
A	293	50	252	0.40	240
B	293	55	246	0.14, 0.60	235
E	293	56	248	0.14, 0.60	235
G	293	30, 65	248	0.36	235
			260	3.2	

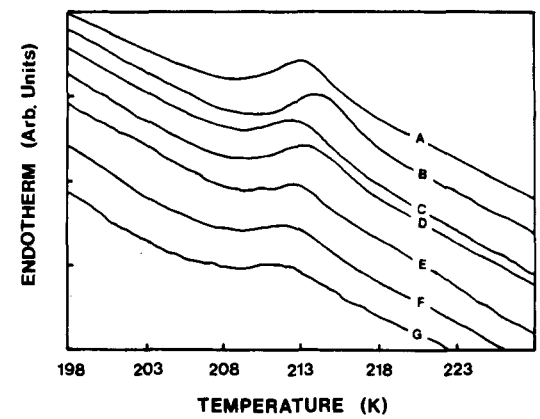

Figure 2. DSC endotherms for samples A–G at a scan rate of 20 °C min^{-1}. The vertical scale differs from one sample to another. Sample H, composed almost entirely of carbon black, did not exhibit a glass transition.

Call's formulas[20,25] ($T_{1(min)}$ = 18 ms and $T_{1\rho(min)}$ = 0.11 ms) is consistent with the anticipated distribution of correlation times in these samples or with anisotropic motion or both.[26] Note also the significant differences in the three relaxation times at high temperatures, which is symptomatic of constrained anisotropic motions in the melt, as observed earlier.

The minor variations in the NMR data for the four samples in Table I and complementary DSC data (Figure 2) reveal at most a modest dependence of T_g on sample treatment. Note that the change in enthalpy, ΔH, associated with the glass transition is proportional to the weight percent of rubber in the samples. The fit is

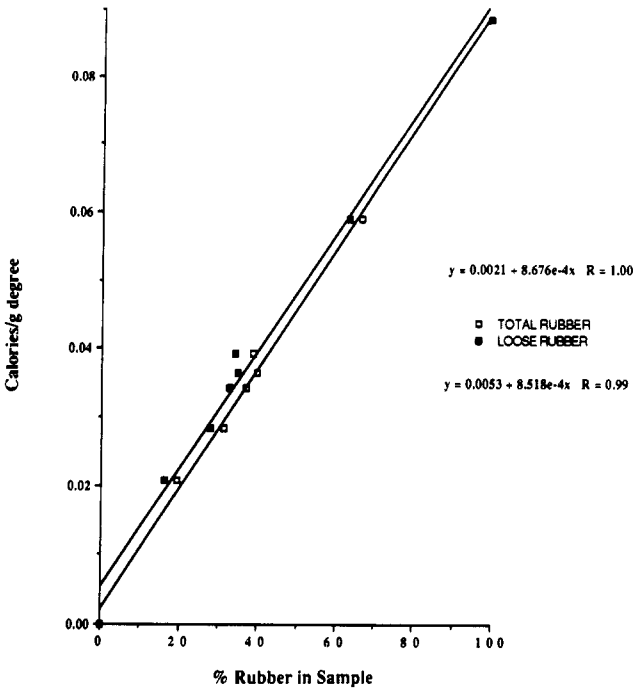

Figure 3. Change in enthalpy, ΔH, at the glass transition as a function of weight percent rubber in the sample: total rubber (□); loosely bound rubber (■) estimated at 293 K. The respective fits are $\Delta H = 0.0021 + 0.00087W$ ($R = 1.00$) and $\Delta H = 0.0053 + 0.00085W$ ($R = 0.99$).

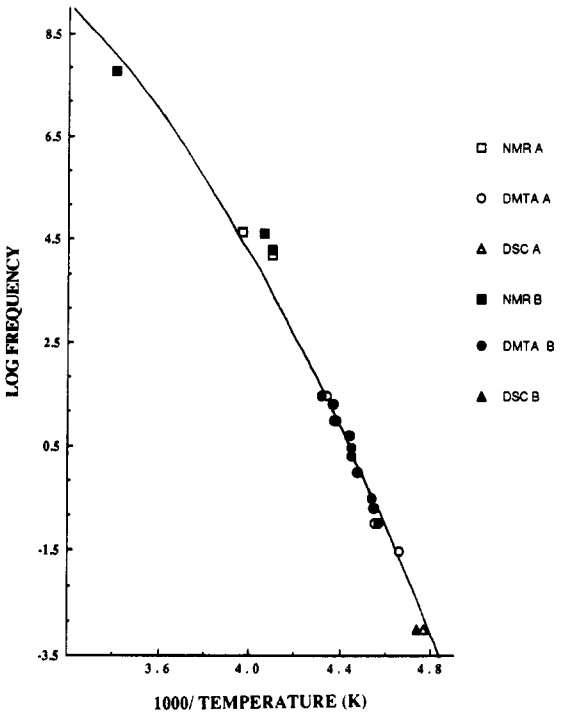

Figure 4. log (correlation frequency) versus $1000/T$ for the glass transition in sample A (unfilled points) and sample B (filled points). NMR (□, ■), DMTA (○, ●), and DSC (△, ▲).

comparably good for ΔH versus weight percent loosely bound rubber (Figure 3). This is in accord with the generally observed insensitivity of DSC to the immobilization of small amounts of tightly bound rubber in the filled elastomer, a view that is reinforced by the results of Figure 4, which compares NMR, DSC, and DMTA relaxation data for samples A and B. Differences in the two sets of results are barely significant, and fits to the WLF expression[27]

$$\log\left(\frac{\nu_1}{\nu_0}\right) = \frac{C_1(T_1 - T_0)}{C_2 + (T_1 - T_0)} \quad (1)$$

yield values of $C_1 = 21.7$ and 20.1 and $C_2 = 81.0$ and 67.0, respectively, for samples A and B. T_g for the filled and unfilled material differs by no more than ~ 1 K.

The temperature dependence of T_1 does not change appreciably from one sample to another, but a shorter component ($I \approx 0.1$–0.2) develops over an increasing temperature range with progression from sample A through G. This nonexponentiality may well reflect the change in the correlation frequency distribution with the relative increase in the amount of more tightly bound material. It may also arise from electron T_1 contributions if the motional spectrum of the electrons in the carbon black embraces sufficiently low correlation frequencies, of the order of 10–100 MHz.

$T_{1\rho}$ is nonexponential in all the filled samples, reflecting, as in earlier studies, the structural and motional heterogeneity of filled elastomers. Justification of the crossover point in the $T_{1\rho}$ curves at ≈260 K rests on the following salient observations.

(i) $T_{1\rho S}$ at the minimum undoubtedly reflects the more loosely bound polymer, characterized by T_{2L}, undergoing its glass transition.

(ii) The suppressed rate of increase in the magnitude of $T_{1\rho S}$ with increasing temperature above the minimum is consistent with the constrained motions of the more tightly bound polymer (assigned unequivocally to T_{2S}). This component will only achieve the liquid-like character, reflected in $T_{1\rho L}$ in the high-temperature regime, when the integrity of the composite structure eventually breaks down. $T_{1\rho S}$ thus appears to be associated with T_{2S} at temperatures above the minimum.

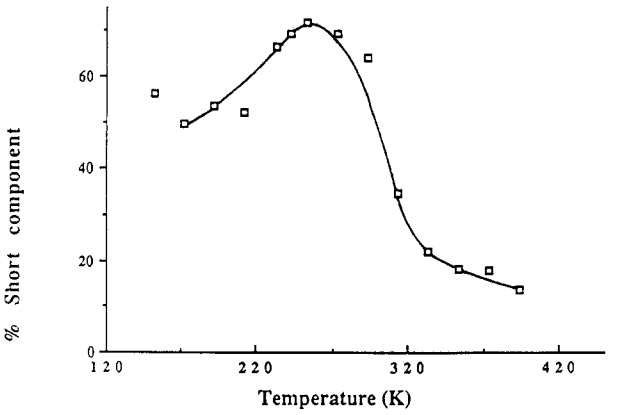

Figure 5. Intensity of the short $T_{1\rho}$, component for sample G as a function of temperature.

(iii) The intensity, $I(T_{1\rho S})$, of the short $T_{1\rho}$ component, typically portrayed for sample G in Figure 5, decreases precipitously to a value comparable to the intensity of T_{2S} at temperatures above the crossover (≈260 K). Note that the effects of spin diffusion, which can appreciably alter $T_{1\rho}$ component intensities,[26] exert minimal influence in the melt because of the reciprocal dependence of the rate of spin diffusion on T_2.

(iv) The pattern of $T_{1\rho}$ relaxation decay at 293 and 348 K, shown in Figure 6 for sample E, reveals that the short T_2 decays first, confirming the view that $T_{1\rho S}$ and T_{2S} components jointly describe the behavior of the more tightly bound polymer at and above room temperature.

From these observations, it is clear that $T_{1\rho S}$ is associated with T_{2L} below ≈260 K and with T_{2S} above, thereby establishing the crossover point. The magnitude of $T_{1\rho S}$ at the minimum remains quite low in all samples, and a transfer of magnetization between the Zeeman and dipolar

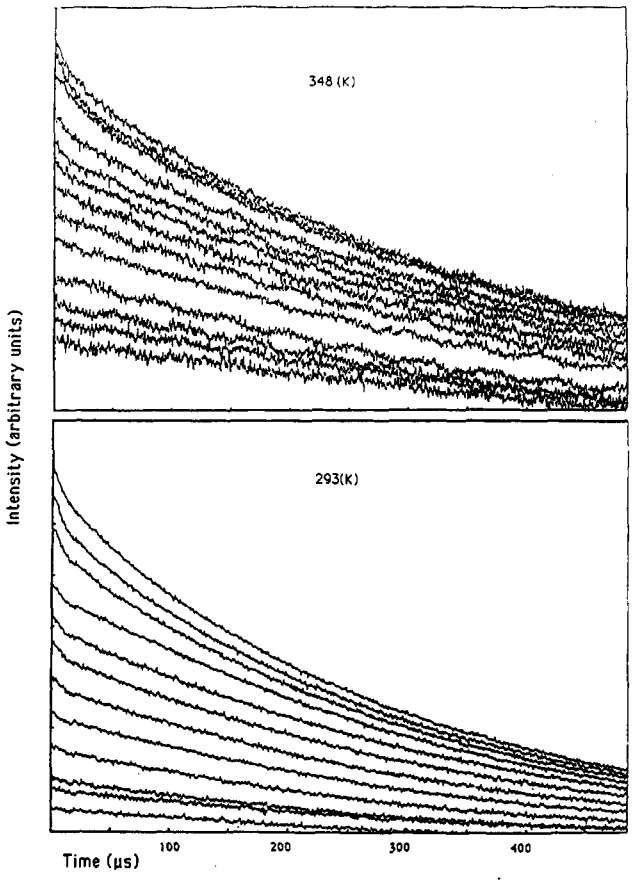

Figure 6. FIDs for sample E at 293 and 348 K for a range of spin-locking times in the rotating-frame experiment. Note that the short T_2 component decays first.

magnetizations cannot be ruled out. Presumably this mechanism would only be important in the immediate vicinity of the minimum. In any event the overall temperature dependence of $T_{1\rho S}$ above the crossover point is consistent with the increasing influence of the more tightly bound rubber with progressive solvent extraction.

Consider now the collated T_2-temperature data in Figure 7. Fitting the component line shapes to the Weibull function yields E values of ~1.3 and ~1.1 for the short and long components, respectively (Figure 8). The short component lies between the Gaussian and Lorentzian line shapes, whereas the long, mobile, component as expected is almost Lorentzian ($E = 1$). The magnitude of T_{2L} above the glass transition progressively decreases for samples A–H, implying a concomitant shift in the motional distribution toward longer correlation times or a situation where magnetic field gradients due to the carbon black particles assume an increasingly important role. Despite possible modification by spin diffusion coupling of the components associated with the two $T_{1\rho}$'s plotted in Figure 1, the shallower $T_{1\rho}$ minimum of sample H has an apparent shift to higher temperature relative to the other samples, indicative of an increase in average correlation time in this more severely treated sample. Presumably the minimum in the $T_{1\rho}$ as a function of extraction severity reflects changes in the formal distribution of correlation times. Such a change in distribution can also explain the changes in shape of the Carr–Purcell decays as a function of sample treatment, as evident in Figures 12 and 13. No irreversible change in T_2 was detected when samples previously heated to 428 K were rerun after a period of weeks, but, as noted below, there are differences in component intensities. The magnitude of T_{2S} for the filled material persists to 428 K, the upper temperature limit of

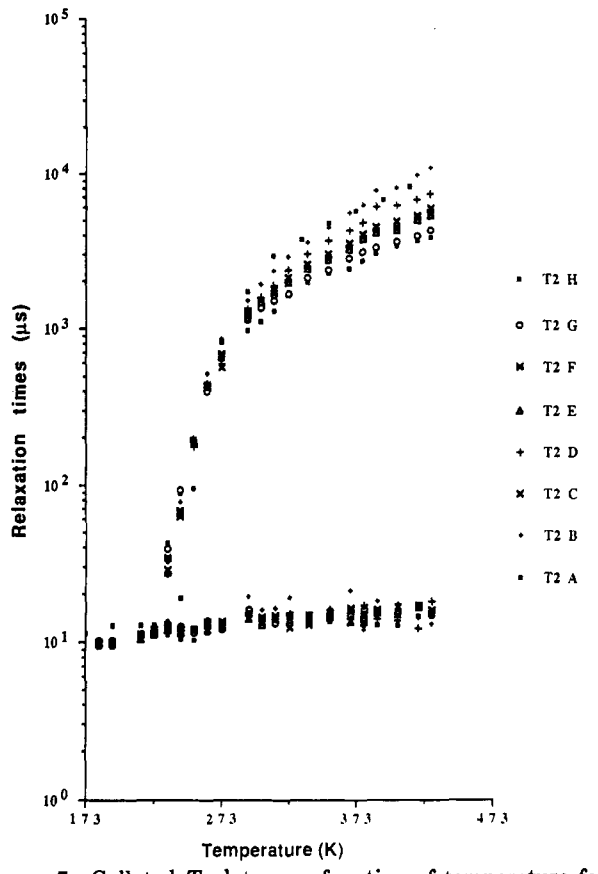

Figure 7. Collated T_2 data as a function of temperature for samples A–H.

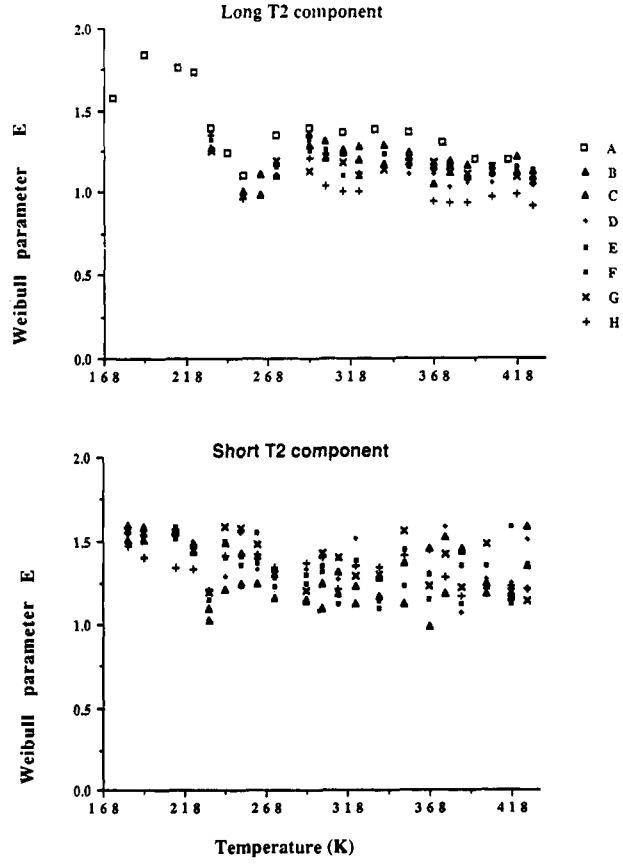

Figure 8. Weibull parameter E as a function of temperature for samples A–H.

this study, and shows no obvious dependence on sample treatment. In a related study, Nishi[28] found an invari-

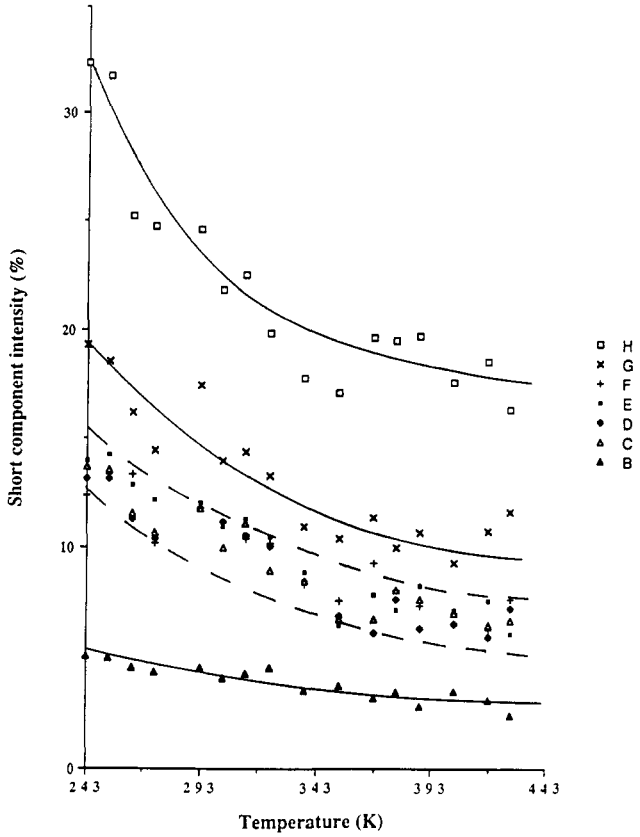

Figure 9. Intensity of the short T_2 component as a function of temperature for samples B–H.

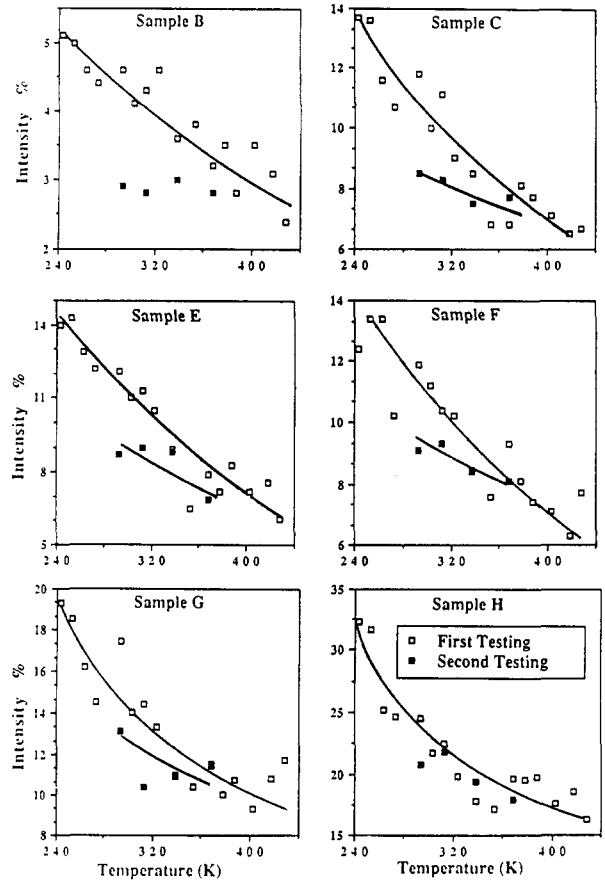

Figure 10. Comparison of $I(T_{2S})$ for successive cycles of T_2 versus increasing temperature: (□) first run; (■) second run.

ance of T_{2S} to changes in concentration of rubber swollen by CCl_4.

The assignment of T_{2S} to the tightly bound layer implies that T_g for the participating elastomer chain elements has increased dramatically, certainly by more than 150 K.[15] Note the modest transition in T_{2S} near 285 K, which, as in earlier studies on *cis*-PB,[15] coincides with the completion of the initial rapid rise in T_{2L} associated with the glass transition. The onset of significant mobility in the more loosely bound phase clearly induces more vigorous motion than would otherwise be the case in the tightly bound layer, thereby revealing cooperation in the chain dynamics between identifiable phases in filled natural rubber.

Component T_2 intensity data presented in Figure 9 are revealing in a number of respects. A general increase in the relative proportion of immobilized or bound layer as the extraction treatment becomes increasingly severe is confirmed. Samples C–F have roughly comparable bound rubber fractions that are appreciably greater than sample A, less than sample G, and significantly less than sample H. As observed earlier,[29] $I(T_{2S})$ decreases with increasing temperature, consistent with the notion of a range of bonding energies between the rubber and carbon black. The amount of bound rubber as reflected in $I(T_{2S})$ correspondingly decreases with increase in temperature as the more energetic molecules overcome their bonding energies and break away from the filler particles. The effects of thermal treatment are not reversible, as the data in Figure 10 reveal: some of the immobilized layer is irreversibly lost, but, interestingly, differences in $I(T_{2S})$ for the two cycles essentially vanish as ~370 K is approached. The effect is much less pronounced in samples G and H. Further annealing of the structure leading to the creation of more mobile polymer may be taking place at temperatures above those used in the initial drying procedure.

In order to explore the dynamics of the intensity–temperature dependence, the data were plotted as ln I versus inverse temperature (Figure 11); the solid lines represent the fit to the expression

$$I(\mathrm{S}) = I_0(\mathrm{S}) \exp\left[\frac{395 \pm 50}{T}\right] \qquad (2)$$

where T is the absolute temperature, $I(\mathrm{S})$ is the observed percent intensity of the short T_2 component, earlier denoted $I(T_{2S})$, and $I_0(\mathrm{S})$ is the intercept on the intensity axis for each of the samples. The magnitudes of $I_0(\mathrm{S})$ are listed in Table II. The mechanism by which the bound rubber molecules are progressively removed with increase in temperature would appear to be Arrhenius in character.

The average thickness of the bound rubber layer, ΔR_0, is computed in the usual way using the Pliskin–Tokita expression[15,30]

$$\mathrm{BR} = \Delta R_0 f\left\{\frac{\phi \rho A}{1-\phi}\right\} + G^i \qquad (3)$$

BR is the fraction of apparently bound rubber, defined as the volume of insoluble polymer divided by the volume of polymer in the composite; f is the fraction of total surface area exposed to the polymer (presumed equal to unity in this study); ϕ is the volume fraction of carbon black in the composite; ρ is the density and A is the specific surface area of the carbon black; and G^i is the fraction of insoluble gel in the unfilled gum.

Thicknesses of the total-bound layer (ΔR_0), listed in Table II, decrease with extraction of increasing severity, which merely reflects a progressive decrease in the overall fraction of bound rubber. Significantly more interesting is the behavior of $I(T_{2S})$ for the extracted samples B–H (Figure 9). For samples C–F the *relative* amounts of tightly and loosely bound rubber do not change appreciably. This

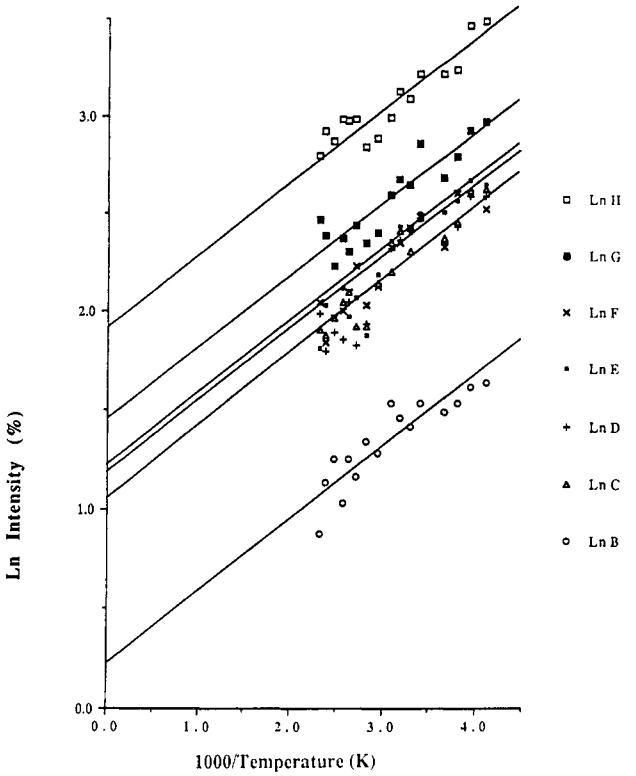

Figure 11. Plot of ln $[I(T_{2S})]$ versus inverse temperature for samples B–H. The intensity $I(T_{2S})$ for each sample is denoted $I(S)$ in eq 2, and $I_0(S)$ is the intercept on the ordinate axis. (See also Table II.)

Table II
Data Relevant to Eqs 2 and 3 (See Text)

sample	$I_0(S)$,[a] %	$I(T_{2S})$,[b] %	bound rubber, vol frac	eff loading,[c] phr	ΔR_0,[d] nm
B	1.3	4.6		(50)	
C	2.9	11.8	0.331	151	8.34
D	2.9	11.8	0.315	158	7.94
E	3.2	12.1	0.295	169	7.43
F	3.4	11.9	0.231	217	5.82
G	4.1	17.4	0.121	413	3.05
H	6.9	24.6			

[a] See eq 2. [b] Room temperature data. [c] 50 phr for sample B relates to the unextracted sample. Remaining data assume no loss of carbon black in the extraction procedure, and these values correspond exactly to the rubber/carbon black ratios given in the Experimental Section. [d] Total thickness of the bound layer.

is consistent with the notion of the removal of chains (folds, cilia, and tie molecules) that are perhaps adsorbed rather than chemically attached to the carbon black particles. Recall that the first few units of a chain attached to a filler particle are characterized by a T_2 commensurate with T_{2S}.[31] Removal of the chain will deplete both loosely and tightly bound polymer. This contrasts with the extraction procedures used to prepare samples G and H, where the increased magnitudes of $I(T_{2S})$ clearly reveal a *preferential* depletion of the loosely bound component. A possible explanation for this observation is as follows: strongly anchored chains may participate in multiple adsorptive links to the filler particle for which a significant part of the chain is within the tightly bound shell described by T_{2S}. These chains survive the earlier extraction procedures, and therefore their contribution proportionately increases, consistent with the experimental observation of higher values for $I(T_{2S})$. Data were not available to evaluate layer thicknesses for sample H.

Because of the observed form of the temperature dependence of the relatively immobile component intensity, as described by eq 2 and Figure 11, it is tempting to parameterize these data in thermodynamic terms. In this case one would consider the composite T_2's to result from two populations, bound and unbound, of polymer segments. Because ΔH is only slightly greater than kT, it seems reasonable to conjecture further that these two populations are always in equilibrium in these experiments and therefore

$$\frac{n_B}{1-n_B} = \frac{I_B}{1-I_B} = e^{\Delta H/RT} e^{-\Delta S/R} \approx I_B \qquad (4)$$

where n_B is the mole fraction of bound polymer. Here, ΔS represents the increase in entropy in going from bound to unbound states, and ΔH the corresponding change in enthalpy.

It is to be expected that the parameters that characterize the polymer going from bound to a liquid environment will parallel those observed for the transition from bound to unbound equilibrium. Within this senario the fact that ΔS, estimated as $\Delta S = -k \ln I(S)$, decreases with increasing severity of extraction removes those polymer segments that would experience the greatest increase in ΔS from attaining a liquid-like environment: those molecules that have less confining environments or those that have "annealed" themselves out of more severely confining situations remain behind. The entropies calculated in this way are reasonably small, consistent with the small enthalpy.

The Carr–Purcell (CP) pulse train[32-39] has been used to explore further the dynamics of molecular motion in a number of systems. As discussed by Mehring,[40] periodic pulsing of a spin system leads to relaxation that is conceptually and practically related to $T_{1\rho}$. The full implications of the Carr–Purcell sequence are complex, and the following observations are necessarily superficial. In general terms, the effects on the T_2 decay of chemical exchange between different sites as monitored by the CP pulse train give additional insight into the way in which resonant nuclei, and therefore the elastomer chains to which they are attached, sample different environments in the filled elastomer. Chemical exchange induces random irreversible dephasing of nuclear moments to an extent that depends upon the time τ_p between successive 180° pulses in the CP sequence[19] or its Meiboom–Gill modification (CPMG):[41,42] as τ_p increases, the number of exchanges increases and therefore T_2 is expected to decrease. Typical T_2 decays recorded at 323 K for CPMG interpulse spacings τ_p within the range 80–400 μs are furnished in Figure 12. Relaxation times and intensities of the shorter mobile component are presented in Figure 13 as a function of τ_p for the range of samples studied. Note in these measurements that T_2 for the immobilized layer remains undetected. Samples are designated in terms of carbon black loading (Table II) in these figures. A number of observations can be drawn:

(i) The magnetization decay is clearly sensitive to τ_p.

(ii) T_2 becomes two component, the longer of which decreases with increasing τ_p as predicted; the effect is more marginal for the shorter mobile T_2 component but the trend is evident.

(iii) There is a marginal decrease in both T_2 components with increased carbon black loading at 293 K. The effect is much more pronounced at 323 K.

(iv) The intensity of the short mobile T_2 component increases with increasing τ_p and with increasing carbon black loading.

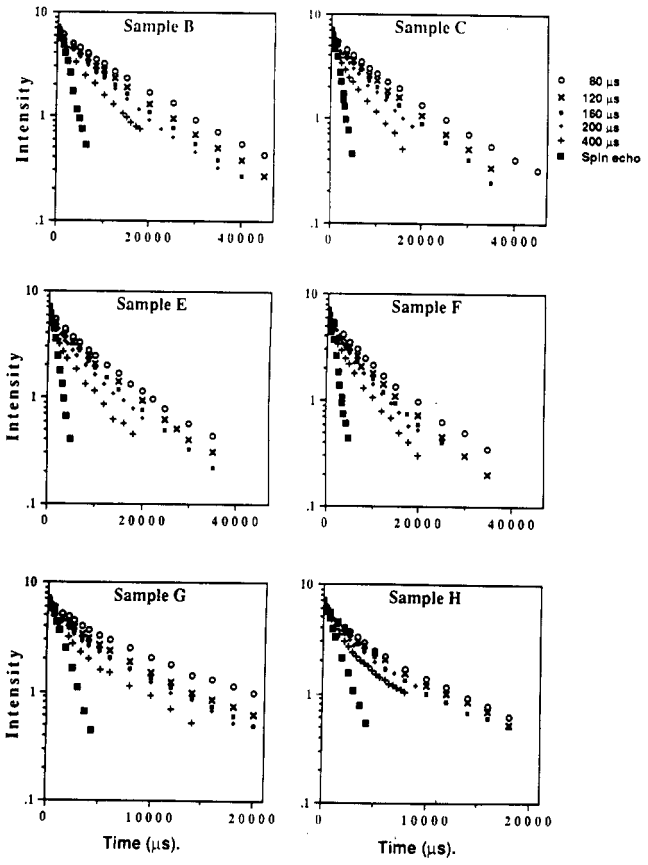

Figure 12. Effect of the interpulse spacing τ_p in the CPMG sequence on the magnetization decay for the samples shown. T = 293 K. Symbols are for various values of τ_p as indicated.

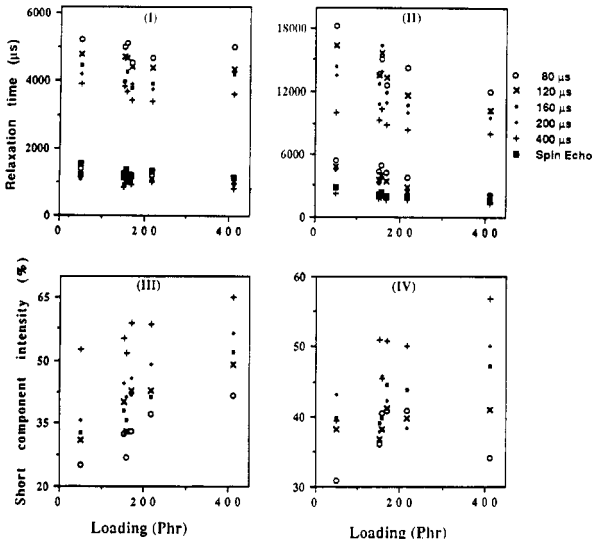

Figure 13. Relaxation times and intensities of the shorter and longer mobile component as a function of τ_p for samples designated according to their carbon black loading (see Table II). Symbols are for various values of τ_p as indicated. I and II, T_2 relaxation times at 293 and 323 K, respectively; III and IV, shorter mobile component intensity at 293 and 323 K, respectively.

The 180° pulses of the CP sequence do not alter the homonuclear dipolar Hamiltonian, which is bilinear in spin, but do, in effect, change the sign of terms linear in the spin, such as chemical shifts and susceptibility effects. At the shortest cycle time the slopes of the CP decays correspond to those expected for limitation by $T_{1\rho}$-like relaxation processes. Therefore, for moderately mobile materials observed in the CP experiment, the major source of local field is residual susceptibility and chemical shift fields rather than residual dipolar fields. The loss of intensity out of the long T_2 is generally consistent with exchange between magnetically heterogeneous sites where a decrease in T_2 as τ_p increases is expected.

The rather convoluted picture emerging from the NMR, DSC, and DMTA data on the extracted samples may be summarized in terms of (a) those results that yield direct information on structure and (b) measurements sensitive to chemical exchange that exploit the Carr–Purcell sequence. The latter have much potential for resolving various contributions to the residual line widths, but only tentative conclusions are indicated here. Their full exploitation requires further detailed theoretical and experimental comparison which will form the basis of future work. Conclusions are more definitive in regard to refinements that can be made to the earlier structural model.[15] In particular, the following may be stated:

(i) There is direct evidence of motional cooperation between the tightly and more loosely bound polymer layers around the filler particles.

(ii) The dependence of T_{2S} intensity data and, concomitantly, the thickness of the bound layer on the severity of extraction and on temperature arises from a range of adhesion energies of polymer to filler.

(iii) The mechanism by which the bound polymer is removed with increasing temperature has Arrhenius character within experimental error. Order of magnitude estimates of entropy ΔS imply that extraction removes those polymer segments that would experience the greatest increase in ΔS by achieving liquid-like character.

Acknowledgment. It is a pleasure to acknowledge the assistance of F. X. Quinn and C. Keely in the acquisition and analysis of DSC and DMTA data, respectively. Discussions and preliminary data acquisition by G. E. Wardell are greatly appreciated.

References and Notes

(1) Kraus, G., Ed. *Reinforcement in Elastomers*; Wiley: New York, 1965.
(2) Rigbi, Z. *Adv. Polym. Sci.* **1980**, *36*, 21.
(3) Schaefer, J. *Macromolecules* **1972**, *5*, 427.
(4) English, A. D.; Dybowski, C. R. *Macromolecules* **1984**, *17*, 446.
(5) English, A. D.; *Macromolecules* **1985**, *18*, 178.
(6) Cohen-Addad, J. P. *J. Chem. Phys.* **1974**, *60*, 2440.
(7) Cohen-Addad, J. P. *J. Phys. (Paris)* **1982**, *43*, 1509.
(8) Cohen-Addad, J. P.; Dupeyre, R. *Macromolecules* **1985**, *18*, 1612.
(9) VanderHart, D. L.; Earl, W. L.; Garroway, A. N. *J. Magn. Reson.* **1981**, *44*, 361.
(10) Komoroski, R. A. *J. Polym. Sci., Polym. Phys. Ed.* **1983**, *21*, 2551.
(11) Schaefer, J.; Chin, S. H.; Weissman, S. I. *Macromolecules* **1972**, *5*, 798.
(12) Dybowski, C. R.; Vaughan, R. W. *Macromolecules* **1975**, *8*, 50.
(13) Cashell, E. M.; Douglass, D. C.; McBrierty, V. J. *Polym. J.* **1978**, *10*, 557.
(14) Kaufman, S.; Slichter, W. P.; Davis, D. D. *J. Polym. Sci., Part A-2* **1971**, *9*, 829.
(15) O'Brien, J.; Cashell, E.; Wardell, G. E.; McBrierty, V. J. *Macromolecules* **1976**, *9*, 653.
(16) Kentgens, A. P. M.; Veeman, W. S.; van Bree, J. *Macromolecules* **1987**, *20*, 1234.
(17) Jeener, J.; Meier, B. H.; Bachmann, P.; Ernst, R. R. *J. Chem. Phys.* **1979**, *71*, 4546.
(18) Powles, J. G.; Mansfield, P. *Phys. Lett.* **1962**, *2*, 58.
(19) Carr, H. Y.; Purcell, E. M. *Phys. Rev.* **1954**, *94*, 630.
(20) McBrierty, V. J. *Polymer* **1974**, *15*, 503.
(21) Weibull, W. *J. Appl. Mech.* **1951**, *73*, 293.
(22) Kaufman, S.; Bunger, D. J. *J. Magn. Reson.* **1970**, *3*, 218.
(23) Hartmann, S. R.; Hahn, E. L. *Phys. Rev.* **1962**, *128*, 2406.
(24) McCall, D. W.; Falcone, D. R. *Trans. Faraday Soc.* **1970**, *66*, 262.
(25) McCall, D. W. *Natl. Bur. Stand. Spec. Publ.* **1969**, *301*, 475.
(26) McBrierty, V. J.; Douglass, D. C. *Phys. Rep.* **1980**, *63*, 61.

(27) Williams, M. L.; Landel, R. F.; Ferry, J. D. *J. Am. Chem. Soc.* **1955**, *77*, 3701.
(28) Nishi, T. *J. Polym. Sci., Polym. Phys. Ed.* **1974**, *12*, 685.
(29) Wardell, G. E.; McBrierty, V. J.; Marsland, V. *Rubber Chem. Technol.* **1982**, *55*, 1095.
(30) Pliskin, I.; Tokita, N. *J. Appl. Polym. Sci.* **1972**, *16*, 473.
(31) Douglass, D. C.; McBrierty, V. J.; Weber, T. A. *J. Chem. Phys.* **1976**, *64*, 1533; *Macromolecules* **1977**, *10*, 178.
(32) Allerhand, A.; Gutowsky, H. S. *J. Chem. Phys.* **1964**, *41*, 2115; **1965**, *42*, 1587.
(33) Bloom, M.; Reeves, L. W.; Wells, E. J. *J. Chem. Phys.* **1965**, *42*, 1615.
(34) Gutowsky, H. S.; Vold, R. L.; Wells, E. J. *J. Chem. Phys.* **1965**, *43*, 4107.
(35) Allerhand, A.; Thiele, E. *J. Chem. Phys.* **1966**, *45*, 902.
(36) Luz, Z.; Meiboom, S. *J. Chem. Phys.* **1963**, *39*, 366.
(37) Carver, J. P.; Richards, R. E. *J. Magn. Reson.* **1972**, *6*, 89.
(38) Jen, J. *J. Magn. Reson*, **1978**, *30*, 111.
(39) Vega, A. *J. Magn. Reson.* **1985**, *65*, 252.
(40) Mehring, M. *High Resolution NMR Spectroscopy in Solids*; Springer-Verlag: Berlin, 1976.
(41) Meiboom, S.; Gill, D. *Rev. Sci. Instrum.* **1958**, *29*, 688.
(42) McBrierty, V. J.; Smyth, G.; Douglass, D. C. *NATO Adv. Study Inst. Ser., Ser. C* **1987**, *198*, 149–160.

Registry No. Hexane, 110-54-3; isooctane, 540-84-1; toluene, 108-88-3; xylenes, 1330-20-7.